

The NNPDF1.2 parton set: implications for the LHC

Alberto Guffanti ¹, Juan Rojo² and Maria Ubiali³

¹ Physikalisches Institut, Albert-Ludwigs-Universität Freiburg
Hermann-Herder-Straße 3, D-79104 Freiburg i. B., Germany

² Dipartimento di Fisica, Università di Milano and INFN, Sezione di Milano,
Via Celoria 16, I-20133 Milano, Italy

³ School of Physics and Astronomy, University of Edinburgh,
JCMB, KB, Mayfield Rd, Edinburgh EH9 3JZ, Scotland

Recently a new set of Parton Distribution Functions (NNPDF1.2) has been produced and released by the NNPDF Collaboration. The inclusion of dimuon data in the analysis allows a determination of the strange content of the proton with faithful uncertainty estimation together with a precision determination of electroweak parameters. In this contribution, we discuss some of the implications of the NNPDF1.2 set, and in particular of its uncertainty determination of the strange PDFs, for LHC phenomenology. First of all, we study the impact on the electroweak boson production cross-section, with special attention to the $\sigma(Z)/\sigma(W)$ ratio. Then we revisit the top pair production cross-section, and perform a comparison of partonic fluxes between various PDF sets. Finally, we discuss the potential of using associated production of W with a charm quark at the Tevatron and the LHC to constrain the proton strangeness.

1 The NNPDF1.2 parton set

The determination of the strange and antistrange quark distributions of the nucleon is considerably interesting from the phenomenological point of view. However, till very recently, the bulk of data included in parton determinations, namely neutral-current deep-inelastic scattering, had minimal sensitivity to flavour separation, and no sensitivity at all to the separation of quarks and antiquark contributions. As a consequence, in standard parton fits the strange and antistrange quark distributions were not determined directly: rather, they were assumed to be equal and proportional to the total light antiquark sea distribution.

Due to the availability of the new deep-inelastic neutrino and anti-neutrino charm production data, which is directly sensitive to the strange and antistrange parton distributions, independent parametrizations of the strange and antistrange distributions have been included in most recent parton fits.

However, the standard method for determining parton distributions, based on fitting the parameters of a fixed functional form, is known to be hard to handle when the experiments are relatively unconstraining. An alternative approach to parton determination which overcomes this difficulty has been developed by the NNPDF Collaboration in a series of papers [1, 2, 3, 4, 5, 6] ^a. The method is based on the use of neural networks for parton parametrization, and a Monte Carlo method supplemented by a suitable training and stopping algorithm for the construction of the parton fit. In this approach, parton distributions are given as a Monte Carlo sample which represents their probability distributions as inferred from the data.

^aSee also Ref. [7] for a series of benchmark comparisons between the NNPDF approach and the standard approach.

Recently, in Ref. [6], a new parton set, NNPDF1.2, was constructed.^b The addition of dimuon data to the global inclusive deep-inelastic scattering dataset, on which the NNPDF1.0 [4] parton set was based, allows a determination of the strange and antistrange distributions with faithful uncertainty estimation.

In Fig. 1 we compare the total strange PDF, $s^+(x, Q_0^2)$, with $Q_0^2 = 2 \text{ GeV}^2$, as determined from the NNPDF1.2 analysis with the results obtained from other parton sets: CTEQ6.6 [8], where an independent parametrization for s^+ is also used, and NNPDF1.0 and CTEQ6.5 [9], where the strange PDFs are fixed to be proportional to the non-strange sea distributions. We observe that in the case of the NNPDF analysis the main effect of releasing the strange parametrization is a substantial enlargement of the error on the s^+ distribution obtained in the NNPDF 1.2 analysis, which remains anyway compatible with the one of the NNPDF 1.0 set. This is not the case for the CTEQ analysis where it can be observed that the s^+ distributions from CTEQ 6.6 and CTEQ 6.5 present substantial differences both in normalizations and in shapes, especially in the intermediate and small- x region.

We refer to Ref. [6] for further details on the NNPDF1.2 parton set and for a detailed description of its implications in the precision determination of electroweak parameters, such as the CKM matrix elements $|V_{cs}|$ and $|V_{cd}|$ and the QCD corrections to the Paschos-Wolfenstein relation.

Our purpose in this contribution is to briefly examine some of the phenomenological implications of the NNPDF1.2 parton set for LHC physics. In particular, we assess the impact on standard candles of the increased uncertainty in the strange PDF as compared to previous determinations.

When comparing results computed using NNPDF sets with the ones obtained using other parton sets, like CTEQ 6.5/6.6, it is important to keep in mind that central values are affected by a systematic uncertainty due to an approximate treatment of heavy flavour contributions. On the other hand, the size of the PDF uncertainties on the same predictions should not be affected by the heavy flavour contribution.

2 Impact of strangeness on LHC standard candles

We begin by comparing results for the total cross-sections for weak bosons production at the LHC ($\sigma(W^\pm)$ and $\sigma(Z)$), obtained using the NNPDF 1.2 set with the ones obtained using CTEQ6.6, NNPDF1.0, CTEQ6.5 and CTEQ6.1 [10] sets. The computation of the cross sections has been performed including NLO QCD corrections using the MCFM^c program. Results are collected in Table 1.

It is interesting to notice that the size of the PDF uncertainties on these observables is very similar among all the different parton sets. This reinforces the observation already done in Ref. [8] that the uncertainty on total cross sections for weak boson production is rather insensitive to the uncertainty on the strange distribution.

We turn then to a study of the sensitivity of the Z/W ratio $r_{ZW} \equiv \sigma_Z / (\sigma_{W^+} + \sigma_{W^-})$ to the uncertainty in the strange distribution. This observable is particularly interesting given that PDF uncertainties are greatly reduced when considering the ratio of two cross-sections, and thus provides an excellent candidate for a measurement of the LHC luminosity. However, in Ref. [8] it was shown that, although the impact of the uncertainties on the W

^bThe NNPDF1.2 set are available in LHAPDF starting from version 5.7.1.

^cNote that our results for CTEQ 6.6 do not coincide with the results presented in Ref. [8] because of the differences in the codes used for the computation of physical observables.

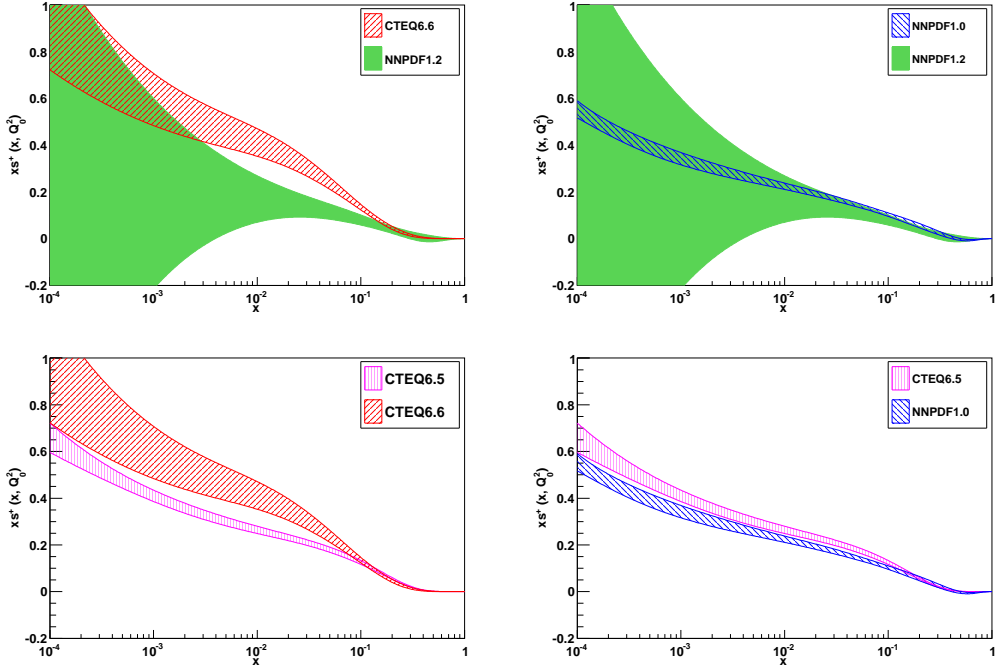


Figure 1: Comparison of the $s^+(x, Q_0^2)$ PDF from various analyses. Upper left plot: NNPDF1.2 vs. CTEQ6.6, where in both cases s^+ is determined from experimental data. Upper right plot: NNPDF1.2, with fitted s^+ vs. NNPDF1.0, with s^+ fixed by flavour assumptions. Lower left plot: CTEQ6.6, with fitted s^+ vs. CTEQ6.5, with s^+ fixed by flavour assumptions. Lower right plot: NNPDF1.0 vs. CTEQ6.5, where in both cases s^+ is fixed by flavour assumptions.

and Z cross sections due to the strange PDF are rather small on their own, the ratio r_{ZW} has a greater sensitivity to the strange uncertainty in the region $0.01 < x < 0.05$ because PDF uncertainties do not completely cancel in the ratio. Therefore, r_{ZW} is potentially affected by the larger uncertainty of strange PDF found in the NNPDF1.2 analysis with respect to other parton densities determinations.

The NNPDF 1.2 prediction for the ratio r_{ZW} and the correlation^d $\rho [\sigma(Z), \sigma(W^\pm)]$ are given in Tab. 2, together with the results obtained using the NNPDF 1.0, CTEQ6.5 and CTEQ 6.6 sets. In the Hessian approach, which is used for the CTEQ sets, the correlation between the two observables considered, $\sigma(W^\pm)$ and $\sigma(Z)$, is computed using the method described in [8]. In the Monte Carlo approach, used for computing PDF uncertainties for the NNPDF sets, the corresponding expression is given, as described in Ref. [4], by

$$\rho [\sigma(Z), \sigma(W^\pm)] = \frac{\langle \sigma(Z) \sigma(W^\pm) \rangle_{\text{rep}} - \langle \sigma(Z) \rangle_{\text{rep}} \langle \sigma(W^\pm) \rangle_{\text{rep}}}{\sqrt{\langle \sigma(Z)^2 \rangle_{\text{rep}} - \langle \sigma(Z) \rangle_{\text{rep}}^2} \sqrt{\langle \sigma(W^\pm)^2 \rangle_{\text{rep}} - \langle \sigma(W^\pm) \rangle_{\text{rep}}^2}} , \quad (1)$$

where the averages are performed over the N_{rep} replicas of the NNPDF sets.

^dRef. [8] instead uses the notation $\cos \varphi$ to denote the correlation between two PDFs/observables.

	$\sigma(W^+) \text{Br}(W^+ \rightarrow l^+ \nu_l)$ [nb]	$\sigma(W^-) \text{Br}(W^- \rightarrow l^+ \nu_l)$ [nb]	$\sigma(Z^0) \text{Br}(Z^0 \rightarrow l^+ l^-)$ [nb]
NNPDF 1.0	11.83 ± 0.26	8.41 ± 0.20	1.95 ± 0.04
NNPDF 1.2	11.99 ± 0.34	8.47 ± 0.21	1.97 ± 0.04
CTEQ6.1	11.65 ± 0.34	8.56 ± 0.26	1.93 ± 0.06
CTEQ6.5	12.54 ± 0.29	9.19 ± 0.22	2.08 ± 0.04
CTEQ6.6	12.41 ± 0.28	9.11 ± 0.22	2.07 ± 0.05

Table 1: The LHC benchmark cross sections for NNPDF1.0 and CTEQ6.5 (with strangeness proportional to the non-strange sea) and NNPDF1.2 and CTEQ6.6 (with strangeness determined from the global analysis). The CTEQ6.1, with a ZM scheme for heavy quarks, is also shown for comparison. All numbers shown are for $\sqrt{s}=14$ TeV. PDF uncertainties correspond to 68% confidence levels.

	NNPDF1.2	NNPDF1.0	CTEQ6.6	CTEQ6.5
r_{ZW}	0.0961 ± 0.0005	0.0965 ± 0.0003	0.0964 ± 0.0004	0.0957 ± 0.0002
$\rho [\sigma(Z), \sigma(W^\pm)]$	0.976	0.994	0.983	0.994

Table 2: Comparison of the values for the ratio of the Z and W cross sections at the LHC as well as their correlation $\rho [\sigma(Z), \sigma(W^\pm)]$, Eq. 1, computed with different PDF sets. Again, all results are computed for a center-of-mass energy of $\sqrt{s}=14$ TeV.

In Fig. 2 we compare the σ_Z - σ_W one sigma correlation ellipses for the NNPDF 1.2, NNPDF 1.0, CTEQ 6.6 and CTEQ 6.5 sets. We note that, despite the fact that the error band on the strange parton densities is in general much larger for the NNPDF 1.2 set than for CTEQ 6.6, the uncertainty on the ratio r_{ZW} is of the same size. This is a consequence of the fact that, as previously mentioned, this ratio is mostly correlated to the strange PDFs in a limited region of x , namely $0.01 < x < 0.05$, where the NNPDF1.2 and CTEQ6.6 uncertainties on s^+ are roughly of the same size. This can be understood as a consequence of the fact that the NuTeV dimuon data, which constrains the strangeness in the two analyses, cover precisely this kinematical range.

The situation could be different if we look at the the differential rapidity distribution. In order to check this, in Fig. 3 we show the rapidity distribution of the ratio r_{ZW} defined as

$$\frac{dr_{ZW}}{dy}(y) \equiv \frac{d\sigma^Z(y)/dy}{d\sigma^W(y)/dy}, \quad (2)$$

together with the associated PDF uncertainties. We observe a sizable increase in the PDF uncertainty for the NNPDF 1.2 result, when compared to results obtained with other sets, at forward rapidities. This is due to the increase of the NNPDF1.2 strange uncertainties at small- x , shown in Fig. 1. However in the central rapidity region, which provides the bulk of the contribution to r_{ZW} , the uncertainties of CTEQ6.6 and NNPDF1.2 turn out to be comparable, confirming the agreement of PDF uncertainties on the integrated ratio shown in Table 2.

3 The $t\bar{t}$ total cross section and partonic fluxes

The total $t\bar{t}$ cross section, $\sigma(t\bar{t})$, has been the subject of several recent studies [8, 11, 12], partially motivated by the possibility of using this process as a standard candle at the LHC to measure the luminosity. To compare the predictions of the NNPDF1.2 set to ones of the other parton determinations, the total $t\bar{t}$ cross section is shown in Fig. 4 for various PDF

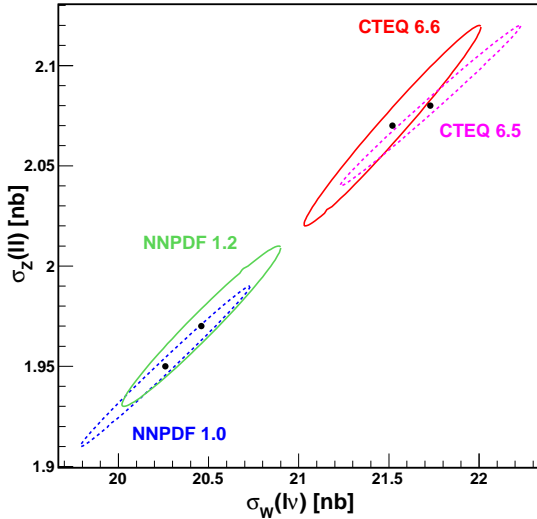


Figure 2: Comparison of the W and Z one sigma correlation ellipses at the LHC obtained from different fits: NNPDF 1.2 (green), NNPDF 1.0 (blue), CTEQ 6.6 (red) and CTEQ 6.5 (purple).

sets.

The computation has been performed with MCFM at NLO. No soft gluon resummation corrections, as done in Ref. [11], are included. All scales are set equal to $m_t = 172.5$ GeV. Together with NNPDF1.2, we show the predictions from NNPDF 1.0 and various other sets from the CTEQ and MRST/MSTW collaborations. It is clear from Fig. 4, comparing for example NNPDF 1.0 and 1.2, or CTEQ 6.5 and 6.6, that strangeness plays a rather minor role for this observable.

In order to understand the results of Fig. 4, one should take into account the fact that the values of $\alpha_s(M_Z^2)$ used each global PDF are different. This is especially important for hadronic cross sections in which the leading order process is a strong interaction process (like in $t\bar{t}$ or $gg \rightarrow H$), since in these cases the cross section at leading order will be proportional to α_s^2 . Moreover, in general there is a correlation between α_s and the PDF uncertainties, mostly the gluon, as discussed for example in Refs. [13, 14]. Note that, while CTEQ 6.6 and NNPDF 1.2 use the value of $\alpha_s(M_Z^2)$ roughly along the lines of the most up-to-date global average ($\alpha_s = 0.118$ and $\alpha_s = 0.119$ respectively), MSTW08 [14] determines it from the PDF analysis ending up with $\alpha_s = 0.1202^{+0.0012}_{-0.0015}$ at NLO.

The use of different values of α_s has to be taken into account when comparing this kind of standard candle processes. For example, the ratio $[\alpha_s^{\text{mstw08}}/\alpha_s^{\text{cteq66}}]^2$, which appears in the Born top pair production cross-section, implies that, even for identical PDFs, the MSTW08 cross-section will be $\sim 4\%$ higher than the CTEQ6.6 one. Therefore, the use of different values of α_s could explain part of the discrepancy between various PDF sets. This emphasizes the importance of using a unique value of the strong coupling for comparison between benchmark observables, especially those proportional to α_s already at leading order.

In order to compare the contributions from each PDF flavour to the total cross-section

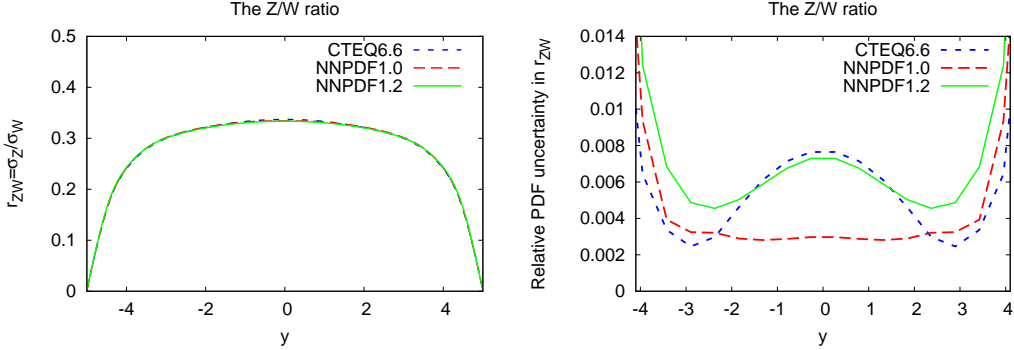


Figure 3: Left: the differential rapidity distribution of the ZW ratio, defined in Eq. 2. The very small PDF uncertainties are not shown. Right: the relative PDF uncertainties in r_{ZW} , as a function of the rapidity y .

for $t\bar{t}$ production we follow the approach of Ref. [15], where the hadronic cross section is written as

$$\sigma(S, m_t^2) = \frac{\alpha_s^2(\mu^2)}{m_t^2} \sum_{ij} \int_0^1 \frac{d\tau}{\tau} \Phi_{ij}(\tau, \mu^2) \tilde{\sigma}_{ij} \left(\frac{\rho^t}{\tau}, \frac{\mu^2}{m_t^2} \right), \quad \rho^t = \frac{4m_t^2}{S}, \quad (3)$$

that is, as a convolution between a partonic cross section $\tilde{\sigma}_{ij}$ and parton fluxes Φ_{ij} , defined as

$$\Phi_{ij}(\tau, \mu^2) = \int_0^1 dx_1 \int_0^1 dx_2 q_i(x_1, \mu^2) q_j(x_2, \mu^2) \delta(x_1 x_2 - \tau), \quad (4)$$

which in turn are convolutions of parton distributions. Note that at the LHC, for $\sqrt{S} = 14$ TeV, for a top quark mass of $m_t = 172.5$ GeV one obtains $\rho^t \sim 6 \cdot 10^{-4}$.

The dominant contribution to top pair production at the LHC comes from the gluon-gluon and gluon-quark channels. In Fig. 5 we show the absolute fluxes for these two channels, as defined in Eq. 4 for $\mu^2 = m_t^2$, for the three most recent PDF sets of the CTEQ, MSTW [16] and NNPDF Collaborations, in the kinematical region relevant for top pair production. The three PDF sets considered agree reasonably well. In order to obtain a more detailed picture of the comparison, in Fig. 6 we show the relative differences between the PDF fluxes for the two channels considered before, using the central CTEQ6.6 result as a reference. We observe a good agreement for the fluxes in the GG channel, as well as for the QG channel in most of the τ range, with the exception of the middle region where a 2σ discrepancy is found. The origin of such discrepancy might be related to differences in the treatment of heavy quark mass effects in NNPDF1.2 compared to the other sets.

Finally, let us compare in more detail the size of PDF uncertainties in the parton fluxes. Following Ref. [17], we compare the relative PDF uncertainties from the fluxes computed with NNPDF1.2, CTEQ6.6 and MSTW08 as a function of $\hat{S} = x_1 x_2 S$. That is, we compute PDF uncertainties in $\Phi_{ij}(\tau = \hat{S}/S, \mu^2)$ as a function of \hat{S} . These parton fluxes have been computed at $\mu^2 = 10^4$ GeV 2 , the typical scale for processes like W, Z or H production at the LHC, again assuming $\sqrt{S} = 14$ TeV.

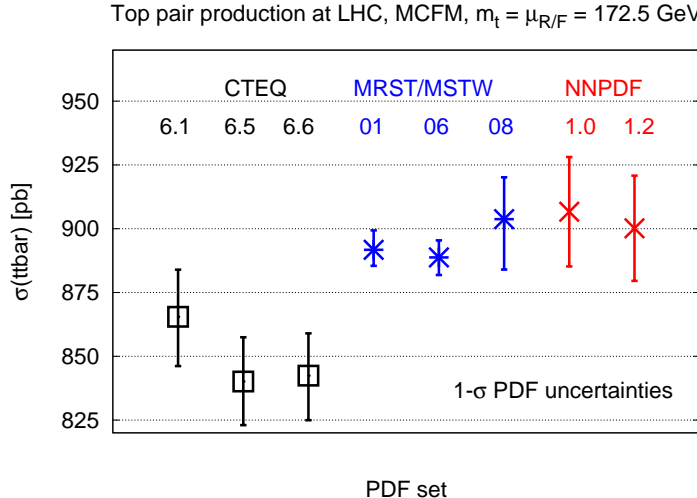


Figure 4: Comparison of the total $t\bar{t}$ cross section computed with recent PDF sets. The computation has been performed with the MCFM program at NLO for $m_t = \mu_R = \mu_F = 172.5$ GeV. All PDF uncertainties correspond to 68% confidence levels.

We show the results of the comparison in Fig. 7. Note that only PDF uncertainties are shown, all central values are set to 1, unlike the case of Fig. 5. We observe a reasonable agreement in the size of PDF uncertainties in the intermediate \hat{S} region, and sizable differences at smaller \hat{S} . In the intermediate \hat{S} region, relevant for the production of massive objects, the PDF uncertainty in the QG channel turns out to be somewhat larger in NNPDF1.2 as compared to both CTEQ6.6 and MSTW08. This could be due to missing hadronic data in the former or to a parametrization bias in the latter: the upcoming NNPDF2.0 global analysis should settle this issue.

4 Wc production and constraining strangeness at the LHC

In the last section of this contribution, we focus on a LHC process which in principle could be used to measure the strange PDF which is presently poorly constrained in the region $x < 10^{-2}$ [6], Wc associated production. The associated production of a vector boson and a charm quark at hadronic colliders is directly sensitive to the strange sea PDF and for this reason, in the past it has been proposed as a candidate for constraining the strange PDF at the TeVatron and the LHC colliders [18].

We revisit this proposal by comparing the NNPDF1.2 predictions for the total Wc cross section with recent measurements at the Tevatron [19] and giving predictions for the LHC.

The dominant production channel for Wc production is $gq \rightarrow Wc$, with q a down-type quark. As in the case of neutrino dimuon production, the down and bottom initiated contributions are suppressed with respect to the strange one by the smallness of the corresponding CKM matrix elements, and therefore at LO, neglecting CKM mixing, the cross section is proportional to the strange PDF.

Associated W and charm production looks therefore like a promising channel for pro-

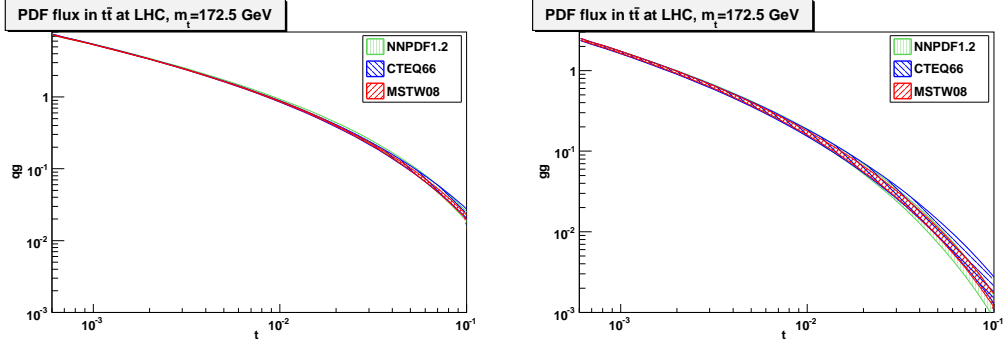


Figure 5: The partonic fluxes, defined in Eq. 4, in the QG (left) and the GG (right) channel, for the NNPDF1.2, CTEQ6.6 and MSTW08 PDF sets. The rapid decrease at large τ reflects the smallness of the PDFs at large x . Note that the partonic fluxes are evaluated at $\mu^2 = m_t^2$.

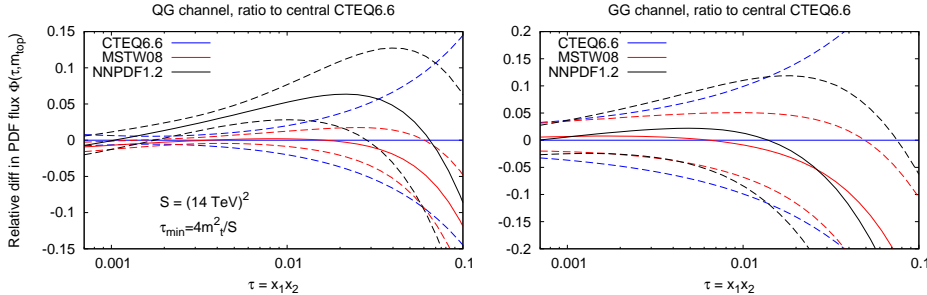


Figure 6: The relative differences between the PDF fluxes in the QG and GG channels between the various sets considered, in the kinematical region relevant for top pair production at the LHC. As in Fig. 5, partonic fluxes are evaluated at $\mu^2 = m_t^2$. Only the kinematically allowed region $\tau \geq \tau_{\min} = 4m_t^2/S$ is shown.

viding a direct constraint on the strange PDF at the energy scale of M_W , two orders of magnitude above the typical energy of the NuTeV dimuon data.

This process has already been studied at the Tevatron. In particular, the CDF experiment has published a measurement of the Wc production cross section, obtained using ~ 1.8 fb^{-1} of $p\bar{p}$ collisions at $\sqrt{s} = 1.96$ TeV. A NLO prediction for this observable can be obtained easily using the MCFM [20] code.

The result obtained by CDF for the measurement of the total cross section is

$$\sigma_{Wc}(p_{Tc} > 20\text{GeV}, |\eta_c| < 1.5) \times \text{BR}(W \rightarrow l\nu) = 9.8 \pm 3.2\text{pb}, \quad (5)$$

which is in agreement with the NLO prediction obtained using MCFM and the NNPDF 1.2 set:

$$\sigma_{Wc}(p_{Tc} > 20\text{GeV}, |\eta_c| < 1.5) \times \text{BR}(W \rightarrow l\nu) = 10.11 \pm 1.24(\text{PDF})^{+0.74}_{-0.92}(\text{scale}) \text{ pb}, \quad (6)$$

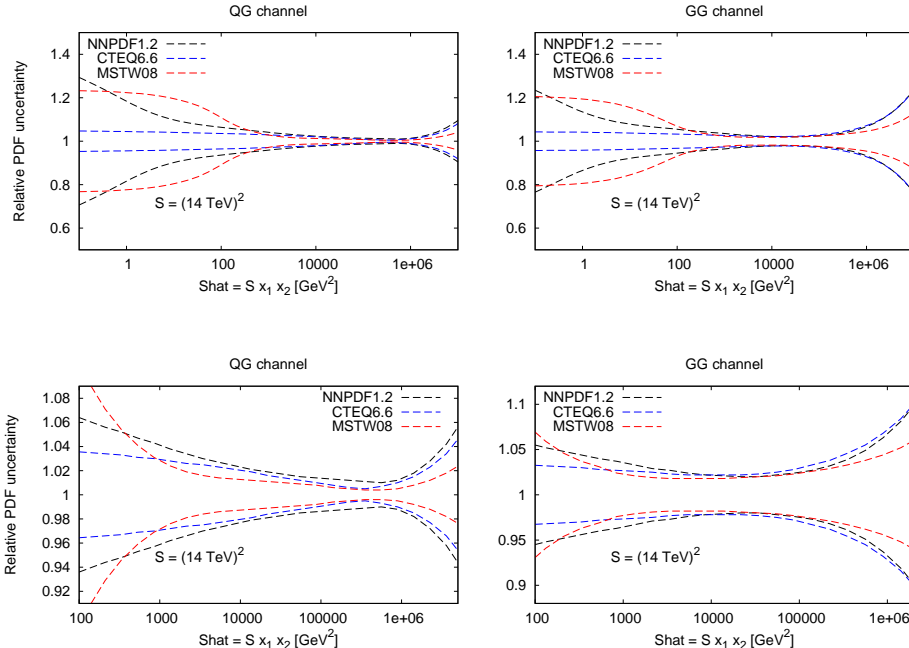


Figure 7: Comparison between the size of PDF uncertainties in the partonic fluxes in the NNPDF1.2, CTEQ6.6 and MSTW08 PDF sets in the region $10^{-5} \leq x \leq 1$ (above) and a zoom in the middle region (below), where PDF uncertainties are smallest. Note that in this case partonic fluxes are evaluated at $\mu^2 = 10^4 \text{ GeV}^2$, as discussed in the text.

where the first error is the one coming from PDF uncertainties and the second one is due to the variation of the renormalization and factorization scales in the perturbative computation. The expected precision of the experimental result, when extrapolated to the full Run II dataset ($\sim 6 - 7 \text{ fb}^{-1}$), is $\sim 15\%$, comparable to the present uncertainty on the theoretical prediction. The theoretical uncertainties at the Tevatron is dominated by PDF uncertainties, with a sizable contribution from scale dependence.

In order to investigate the possibility of using this very same channel as a strangeness constraint at the LHC, we also computed the W_c cross section for the LHC assuming a center of mass energy of 14 TeV and standard rapidity and transverse momentum cuts both for the charm quark and the leptons coming from the W decay. The result that we obtain is

$$\sigma_{W_c}(p_{Tc} > 20 \text{ GeV}/c, |\eta_c| < 4.) \times \text{BR}(W \rightarrow l\nu) = 631 \pm 46(\text{PDF})^{+38}_{-63}(\text{scale}) \text{ pb}. \quad (7)$$

Our result shows that the uncertainty on the theoretical prediction due to scale variations, and thus to higher order corrections, is comparable to the uncertainty due to the strange PDFs. The result seems to suggest that it might be difficult to use this process to constrain PDFs. It might instead be useful to look at differential distributions, like the W or c -jet rapidity or transverse momentum distributions. In any case, unless scale uncertainties can be reduced by higher order computations, the theoretical error limits the usefulness of

Wc production as a constraint for the strangeness distributions, regardless the accuracy of present and future experimental measurements of this channel.

5 Outlook

In this contribution we reviewed some phenomenological implications of the NNPDF1.2 parton set for LHC physics, with emphasis on those observables more directly sensitive to the strange PDFs. A more detailed study of the phenomenological implications of the NNPDF approach to LHC observables is however postponed until the release of the upcoming NNPDF2.0 global parton analysis, which includes all relevant hadronic data like Drell-Yan pair production, vector boson production and inclusive jet production.

Acknowledgments We would like to thank A. Vicini and G. Ridolfi for providing us their code for the computation of the Drell-Yan process and M. Cacciari for useful comments. J.R. thanks the hospitality of the CERN TH division where part of this work was completed. M. U. is founded by a SUPA graduate studentship.

References

- [1] S. Forte, L. Garrido, J. I. Latorre, and A. Piccione, “Neural network parametrization of deep-inelastic structure functions,” *JHEP* **05** (2002) 062, [hep-ph/0204232](#).
- [2] **NNPDF** Collaboration, L. Del Debbio, S. Forte, J. I. Latorre, A. Piccione, and J. Rojo, “Unbiased determination of the proton structure function $f_2(p)$ with faithful uncertainty estimation,” *JHEP* **03** (2005) 080, [hep-ph/0501067](#).
- [3] **NNPDF** Collaboration, L. Del Debbio, S. Forte, J. I. Latorre, A. Piccione, and J. Rojo, “Neural network determination of parton distributions: The nonsinglet case,” *JHEP* **03** (2007) 039, [arXiv:hep-ph/0701127](#).
- [4] **NNPDF** Collaboration, R. D. Ball *et al.*, “A determination of parton distributions with faithful uncertainty estimation,” *Nucl. Phys.* **B809** (2009) 1–63, [arXiv:0808.1231 \[hep-ph\]](#).
- [5] **NNPDF** Collaboration, J. Rojo *et al.*, “Update on Neural Network Parton Distributions: NNPDF1.1,” [arXiv:0811.2288 \[hep-ph\]](#).
- [6] **NNPDF** Collaboration, R. D. Ball *et al.*, “Precision determination of electroweak parameters and the strange content of the proton from neutrino deep-inelastic scattering,” [arXiv:0906.1958 \[hep-ph\]](#).
- [7] M. Dittmar *et al.*, “Parton Distributions,” [arXiv:0901.2504 \[hep-ph\]](#).
- [8] P. M. Nadolsky *et al.*, “Implications of CTEQ global analysis for collider observables,” *Phys. Rev.* **D78** (2008) 013004, [arXiv:0802.0007 \[hep-ph\]](#).
- [9] W. K. Tung *et al.*, “Heavy quark mass effects in deep inelastic scattering and global QCD analysis,” *JHEP* **02** (2007) 053, [arXiv:hep-ph/0611254](#).
- [10] J. Pumplin *et al.*, “New generation of parton distributions with uncertainties from global QCD analysis,” *JHEP* **07** (2002) 012, [arXiv:hep-ph/0201195](#).
- [11] M. Cacciari, S. Frixione, M. L. Mangano, P. Nason, and G. Ridolfi, “Updated predictions for the total production cross sections of top and of heavier quark pairs at the Tevatron and at the LHC,” *JHEP* **09** (2008) 127, [arXiv:0804.2800 \[hep-ph\]](#).
- [12] N. Kidonakis and R. Vogt, “The Theoretical top quark cross section at the Tevatron and the LHC,” *Phys. Rev.* **D78** (2008) 074005, [arXiv:0805.3844 \[hep-ph\]](#).
- [13] J. Pumplin, A. Belyaev, J. Huston, D. Stump, and W. K. Tung, “Parton distributions and the strong coupling: CTEQ6AB PDFs,” *JHEP* **02** (2006) 032, [arXiv:hep-ph/0512167](#).
- [14] A. D. Martin, W. J. Stirling, R. S. Thorne, and G. Watt, “Uncertainties on α_S in global PDF analyses,” [arXiv:0905.3531 \[hep-ph\]](#).

- [15] P. Nason, S. Dawson, and R. K. Ellis, “The Total Cross-Section for the Production of Heavy Quarks in Hadronic Collisions,” *Nucl. Phys.* **B303** (1988) 607.
- [16] A. D. Martin, W. J. Stirling, R. S. Thorne, and G. Watt, “Parton distributions for the LHC,” [arXiv:0901.0002 \[hep-ph\]](https://arxiv.org/abs/0901.0002).
- [17] J. M. Campbell, J. W. Huston, and W. J. Stirling, “Hard interactions of quarks and gluons: A primer for LHC physics,” *Rept. Prog. Phys.* **70** (2007) 89, [arXiv:hep-ph/0611148](https://arxiv.org/abs/hep-ph/0611148).
- [18] H. L. Lai *et al.*, “The Strange Parton Distribution of the Nucleon: Global Analysis and Applications,” *JHEP* **04** (2007) 089, [arXiv:hep-ph/0702268](https://arxiv.org/abs/hep-ph/0702268).
- [19] **CDF** Collaboration, T. Aaltonen *et al.*, “First Measurement of the Production of a W Boson in Association with a Single Charm Quark in Proton Anti-proton Collisions at $\sqrt{s}=1.96$ TeV,” *Phys. Rev. Lett.* **100** (2008) 091803, [arXiv:0711.2901 \[hep-ex\]](https://arxiv.org/abs/0711.2901).
- [20] *MCFM*. <http://mcfm.fnal.gov>. <http://mcfm.fnal.gov>.